JACS
JOURNAL OF THE AMERICAN CHEMICAL SOCIETY
Article
pubs.acs.org/JACS

Modeling Linear and Cyclic PKS Intermediates through Atom Replacement

Gaurav Shakya,[†,§] Heriberto Rivera, Jr.,[‡,§] D. John Lee,[‡] Matt J. Jaremko,[‡] James J. La Clair,[‡] Daniel T. Fox,[‡] Robert W. Haushalter,[‡] Andrew J. Schaub,[†] Joel Bruegger,[†] Jesus F. Barajas,[†] Alexander R. White,[†] Parminder Kaur,[†] Emily R. Gwozdziowski,[‡] Fiona Wong,[†] Shiou-Chuan Tsai,*[,†] and Michael D. Burkart*[,‡]

[†]Departments of Molecular Biology and Biochemistry, Chemistry, and Pharmaceutical Sciences, University of California, Irvine, California 92697, United States

[‡]Department of Chemistry and Biochemistry, University of California, San Diego, 9500 Gilman Drive, La Jolla, California 92093-0358, United States

Supporting Information

ABSTRACT: The mechanistic details of many polyketide synthases (PKSs) remain elusive due to the instability of transient intermediates that are not accessible via conventional methods. Here we report an atom replacement strategy that enables the rapid preparation of polyketone surrogates by selective atom replacement, thereby providing key substrate mimetics for detailed mechanistic evaluations. Polyketone mimetics are positioned on the actinorhodin acyl carrier protein (actACP) to probe the underpinnings of substrate association upon nascent chain elongation and processivity. Protein NMR is used to visualize substrate interaction with the actACP, where a tetraketide substrate is shown not to bind within the protein, while heptaketide and octaketide substrates show strong association between helix II and IV. To examine the later cyclization stages, we extended this strategy to prepare stabilized cyclic intermediates and evaluate their binding by the actACP. Elongated monocyclic mimics show much longer residence time within actACP than shortened analogs. Taken together, these observations suggest ACP-substrate association occurs both before and after ketoreductase action upon the fully elongated polyketone, indicating a key role played by the ACP within PKS timing and processivity. These atom replacement mimetics offer new tools to study protein and substrate interactions and are applicable to a wide variety of PKSs.

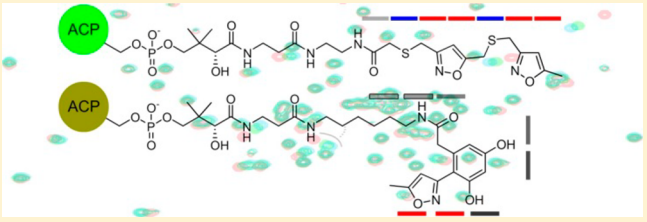

Synthetic mimics of complex natural products are important tools to evaluate the mechanisms of natural product biosynthesis and to access syntheses that diversify the natural product templates. For example, the advent of the Stork−Eschenmoser hypothesis[1] was a defining moment in terpene biosynthesis that enabled synthetic mimickry[2,3] to help elucidate the mechanisms of terpene biosynthesis.[4] Comparable intermediates in aromatic polyketide biosynthesis have not been possible due to the instability of nascent polyketones, hindering advancement in the study of PKS mechanisms, timing, and processivity.[5] Here we describe an approach for generating polyketide intermediates via atom replacement to mimic elongation intermediates in iterative (type II) polyketide synthases. We demonstrate application of these probes to evaluate the biosynthesis of actinorhodin,[6] showing that these materials can mimic partially elongated and cyclized substrates attached to the actACP[7] through analysis of intermediate association.

Figure 1 depicts the proposed biosynthesis of actinorhodin (**1**). Few intermediates within this pathway have been identified,[5] leading to uncertainties in both the succession and process of elongation, reduction, and ring closure. Current structural evidence suggests that the process is dictated by stabilizing residues within binding pockets of corresponding synthases,[8] but this remains hypothetical. Important questions remain to be addressed, including: Why must chain elongation reach full length before reduction and cyclization? How is site-specific carbonyl reduction achieved? Are linear polyketones sequestered by the ACP during chain elongation? Access to elongated, polar mimics of ketide intermediates, such as **4**−**6** (Figure 1), could enlighten these uncertainties by their study in complex with PKS proteins for binding, stabilization, and chain transfer.

Although triketone units can be adapted synthetically, as demonstrated by Barrett[9a−c] and Harris,[9d,e] preparation and study of these and longer polyketones have been impeded by inherent reactivity through spontaneous intra- and intermolecular Aldol/Claisen condensations. We identified a practical solution to this problem by replacing select carbonyls with sulfur atoms, thereby thwarting spontaneous condensation and at the

Received: July 1, 2014
Published: November 19, 2014

   dx.doi.org/10.1021/ja5064857 | J. Am. Chem. Soc. 2014, 136, 16792−16799

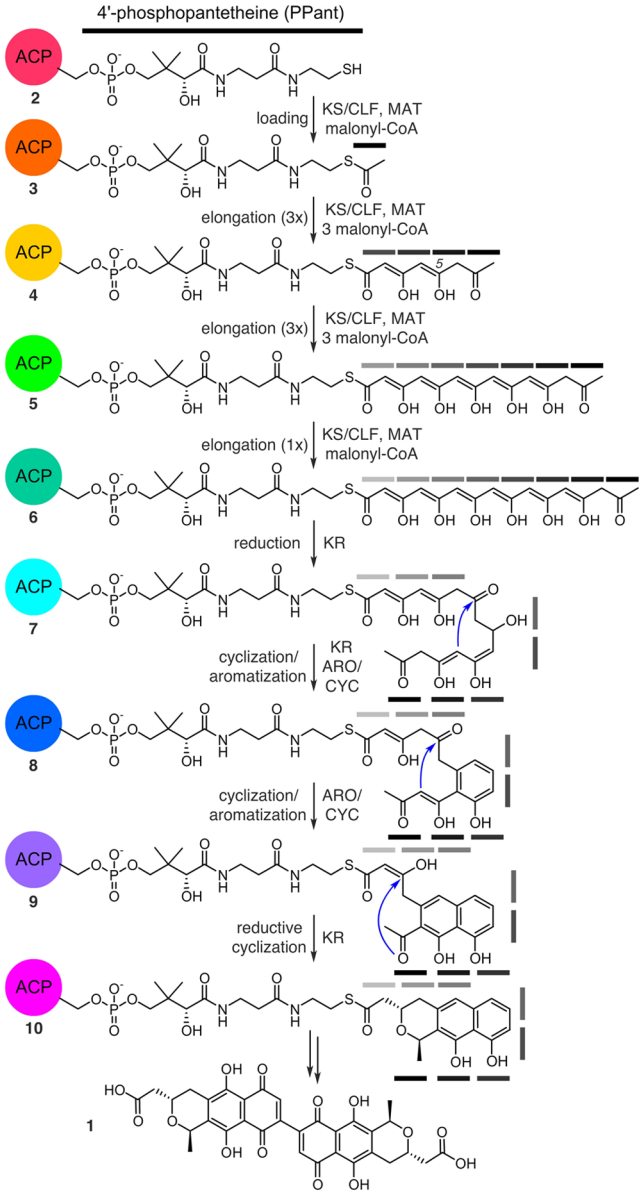

Figure 1. Proposed biosynthesis of **1** from *holo*-actACP (**2**). One depiction of the enol/ketol tautomerization states has been shown, in reality, multiple states likely exist. Gray bars denote ketide units.

same time providing probes to study the effects of length, polarity, and hydrophobicity upon the PKS elongation and cyclization process. We strategically substituted carbonyl groups nonessential for cyclization and/or reduction with sulfur atoms or isoxazole rings and validated their design via docking simulations of the probes upon actACP (Supporting Information). As shown in Figure 2, the corresponding thioethers would serve as a chemical "knockout" of the reactive carbonyl moieties. These probes differ from previously published analogs with the inclusion of both polyketide mimics and the full 4′-phosphopantetheine moiety, thus allowing us to evaluate the significance of ACP−probe interactions. In addition, this atom replacement design offers the added benefit of facile transformation to sulfoxides or sulfones, offering the ability to install greater polarity into the same parent compound.

We began by targeting an atom replacement mimetic of the ACP species bearing tetraketide unit **4** (Figure 1). Of the four carbonyl groups, the third ketide, as shown in **4a** (blue bar,

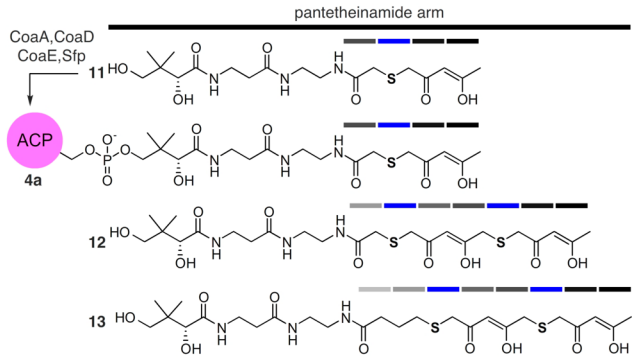

Figure 2. Structures of S atom replaced *crypto*-C8-actACP (**4a**). In this design, select carbonyl groups are replaced by S atoms, therein reducing number of potential Aldol/Claisen condensations. Access to **4a** was achieved by chemoenzymatic conversion of mimetic **11** to its corresponding CoA analog by the action of three *E. coli* enzymes CoaA, CoaD, CoaE followed by loading on the actACP by Sfp (see Supporting Information).[10−12] Mimetics **12** and **13** and their corresponding *crypto*-loaded ACPs were not achieved due to instability. While the installation of the thioethers in **12** and **13** eliminated select Aldol/Claisen condensations, it did not ablate it. Ketide units are denoted by bars and are colored according to replacement of the carbonyl group with S atom (blue).

Figure 2), was selected for replacement. This involved the preparation of tetraketide mimetic **11** (Figure 2), which would be appended onto the actACP using chemoenzymatic methods developed in our laboratories.[11,12] After exploring multiple approaches, we identified a route using an isoxazole as a tool to install a protected diketone unit.[13] As shown in Scheme 1,

Scheme 1. Synthesis of Tetraketide Mimetic 11[a]

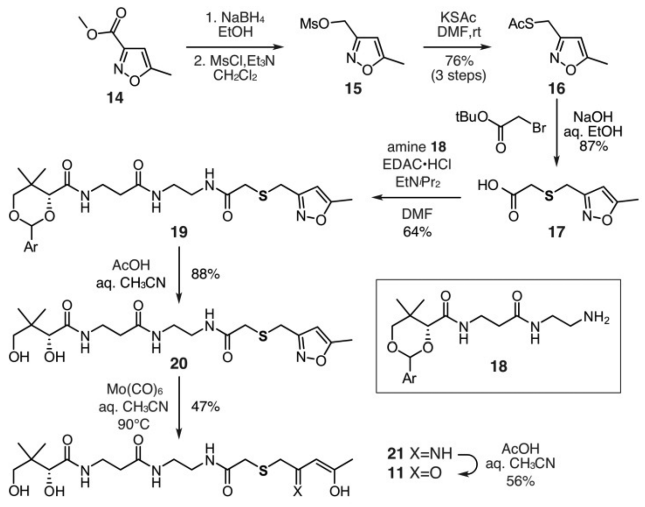

[a]Ar = 4-methoxybenzyl.

mimetic **11** was prepared through an eight-step route that began with commercially available isoxazole **14**. Reduction of **14** and subsequent mesylation afforded **15**, which was converted to thioacetate **16** over the three steps.

Thioacetate **16** was then converted into acid **17** by a three-step one-pot reaction sequence that began with deacetylation of the thioacetal, alkylation of the incipient thiolate, and ester hydrolysis (Scheme 1). Alternatively, addition of thioglycolic acid to mesylate **15** also provided acid **17** (not shown, see Supporting Information). Acid **17** was then coupled to

dx.doi.org/10.1021/ja5064857 | J. Am. Chem. Soc. 2014, 136, 16792−16799

protected-pantetheinamine **18** using conventional EDAC coupling conditions to afford amide **19**. The synthesis of mimetic **11** was completed in three steps by removal of *p*-methoxyphenylacetal using aq. AcOH, opening of the isoxazole in **20** by treatment with $Mo(CO)_6$ in refluxing aq. CH_3CN, and conversion of **21** to **11** by treatment with $AcOH:H_2O:CH_3CN$ (2:2:1). Using this route, we prepared **11** from isoxazole **14** in 10% overall yield over eight steps.

We then turned our attention to examination of mimetics bearing chain-elongated ketides as illustrated by heptaketide **12** and octaketide **13** (Figure 2). Our goal was to compare the short *crypto*-C8-actACP **4a** to the longer *crypto*-C14 or C16 actACPs as a means to validate the chain length specificity during extension of the ketide chain. We began by evaluating the synthesis of **12** and **13** (Figure 2). As depicted in Scheme 2, the

Scheme 2. Synthesis of Chain Elongated Mimetics, Heptaketide 22 and Octaketide 23[a]

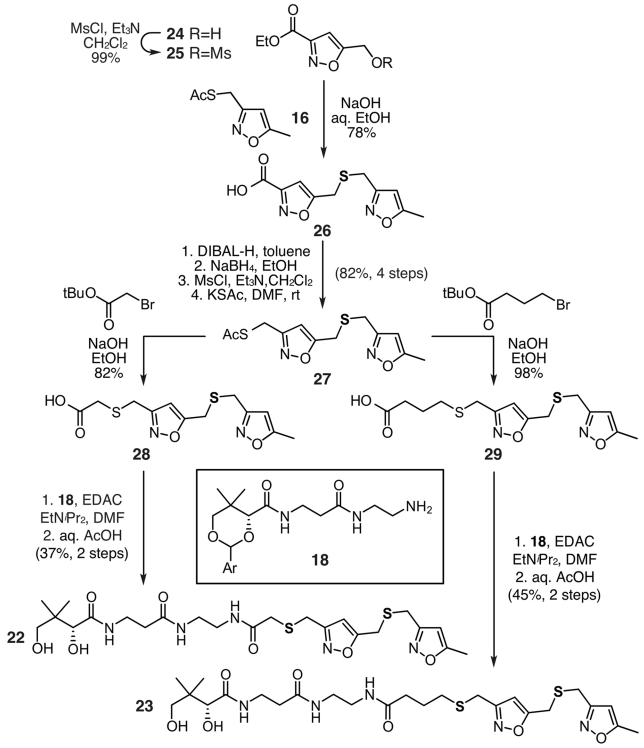

[a]Ar = 4-methoxybenzyl.

synthesis of **12** began by converting isoxazole **24** to its mesylate **25** and coupling it to **16** using our tandem three-step coupling process, as illustrated for the elaboration of **16** to **17** (Scheme 1). The resulting bis-isoxazole-acid **26** was then converted into its corresponding thioacetate **27** in four steps. Again using the tandem three-step coupling process, we were able to access acid **28** in high yield from **27**. The resulting acid **28** was coupled to protected pantetheinamine **18**, which after deprotection, afforded heptaketide **22** in nine steps from **16** and **24** in 19% overall yield. Unfortunately, while multiple conditions and methods were screened, the conversion of **22** (Scheme 1) to **12** (Figure 2) via isoxazole ring opening underwent rapid condensation providing an intractable mixture.

Comparable complications arose in efforts to prepare mimetic **13** (Figure 2). Using thioacetate **27** as a central intermediate, preparation of **13** required only modification of the alkylating agent. Conversion of **27** to **29** was readily achieved using *t*-butyl 4-bromobutanoate (Scheme 2). Coupling acid **29** to **18**, followed by deprotection, completed access to octaketide mimetic **23** in nine steps from **16** and **24** in 28% overall yield. Isoxazole opening in **23** again led to an intractable mixture of products. This indicated that stable mimetics required additional atom replacement.

Fortunately, the solution arose from **20** (Scheme 1), **22** (Scheme 2), and **23** (Scheme 2). Here, the isoxazole motif not only served as a synthetic tool but also provided a second type of atom replacement (Figure 3). In this dual atom replaced model,

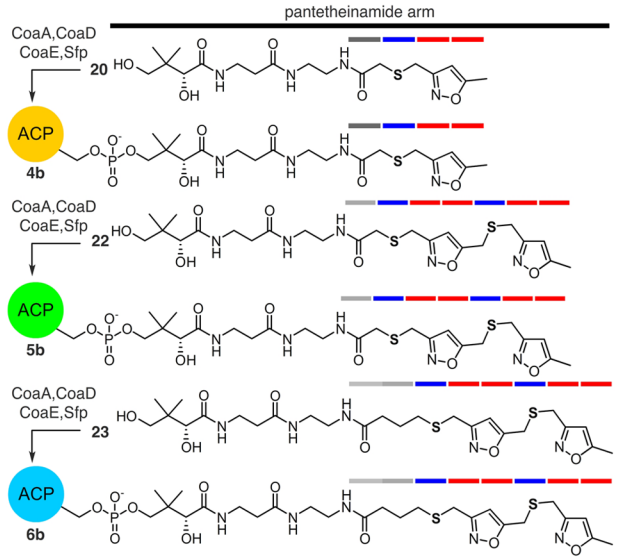

Figure 3. Structures of dual atom replaced *crypto*-C8-actACP **4b**, *crypto*-C14-actACP **5b**, and *crypto*-C16-actACP **6b**. Access to **4b**, **5b**, and **6b** was accomplished by chemoenzymatic attachment of **20** (Scheme 1), **22** (Scheme 2), and **23** (Scheme 2), respectively, to the actACP.[10−12] Ketide units are denoted by bars and are colored according to replacement of a carbonyl with a sulfur atom (blue) or replacement of diketide unit with isoxazole (red).

both carbonyl and dicarbonyl units are replaced with thioether and isoxazole units, respectively. Unlike mimetics **12** and **13**, long chain analogs such as **22** and **23** are readily accessed and are stable, due to their inability to undergo intramolecular Aldol/Claisen condensations.

We applied these atom replacement mimetics to study actACP substrate sequestration as detected by solution-phase protein NMR.[12,14] We appended mimetics **11**, **20**, **22**, and **23** to *apo*-actACP forming the corresponding *crypto*-C8-actACP **4a** (Figure 2), *crypto*-C8-actACP **4b** (Figure 3), *crypto*-C14-actACP **5b** (Figure 3), and *crypto*-C16-actACP **6b** (Figure 3).[12] We then examined samples of proteins **4a**, **4b**, **5b**, and **6b** by solution-phase $^1H,^{15}N$-HSQC NMR (Figure 4a,c).[10] Comparison of *crypto*-C8-actACP **4a** and isoxazole-containing *crypto*-C8-actACP **4b** to *holo*-actACP via chemical shift perturbation (CSP) returned only very slight perturbations, indicative of a substrate that is mostly solvent exposed and not sequestered on the NMR time scale (Figure 4b).[12] These results compare favorably to known analog sequestration, where early intermediates (C6 and smaller) have been shown to not sequester.[14c]

Octaketide **6b** shows ∼30% larger CSPs over **5b** in these key residues, suggesting that the longer substrate, which mimics the fully mature octaketide polyketone in **6**, displays longer

dx.doi.org/10.1021/ja5064857 | J. Am. Chem. Soc. 2014, 136, 16792−16799

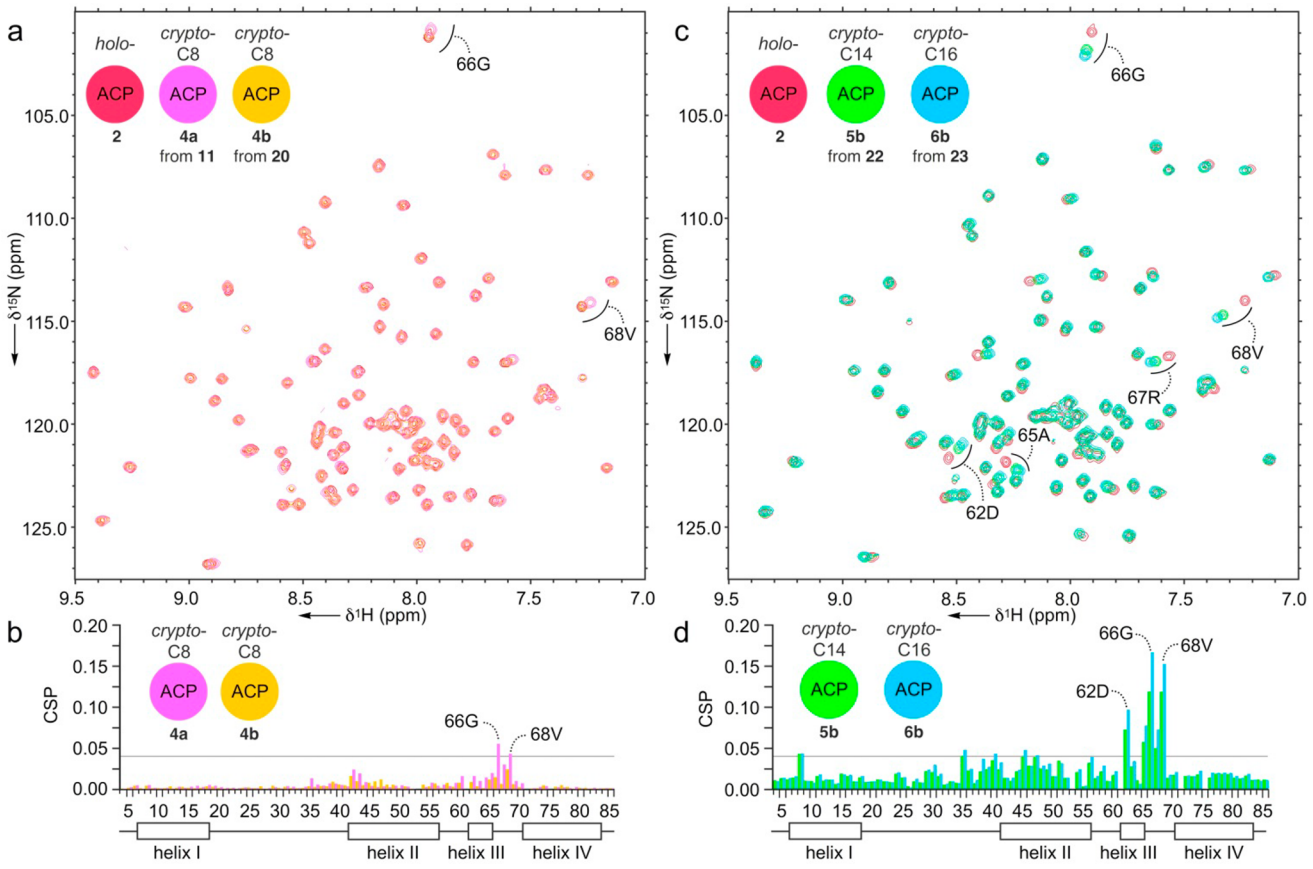

Figure 4. Sequestration analysis of atom replaced mimetics. (a) $^{1}H,^{15}N$-HSQC overlays depicting the *holo*-actACP (**2**, red) and the *crypto*-C8-actACP (**4a**, pink), *crypto*-C8-actACP (**4b**, orange) bearing **11** and **20**, respectively. (b) CSP plots obtained from the spectra shown in panel (a). (c) $^{1}H,^{15}N$-HSQC traces depicting overlays of the *holo*-actACP (**2**, red), *crypto*-C14-actACP (**5b**, green) bearing heptaketide mimetic **22** and *crypto*-C16-actACP (**6b**, blue) bearing the octaketide mimetic **23**. (d) CSP plots obtained from the spectra shown in panel (c). The docked actACP structure with these probes can be found in Figure S34.

residency within the hydrophobic cleft. This pocket is delineated by CSPs found in the same residues of actACP previously reported to stabilize aromatic product analogs.[12] Minimal CSPs for **4a** and **4b** indicate that tetraketide intermediates are not stabilized by interaction with the actACP, likely favoring further elongation by the actKS/CLF. This supports the hypothesis that sequestration of the elongating polyketone is driven by the comparative energetic stability between the ACP sequestered substrate and the ACP-KS/CLF complex. These studies suggest that the mature polyketone is stabilized through association by the hydrophobic cleft formed by movement of helix III of actACP during chain elongation.

Next we turned to evaluate the latter, cyclized intermediates, **7**−**10** (Figure 1), proposed in the biosynthesis of actinorhodin (**1**). We realized that this atom replacement methodology could be uniquely extended for the study of the cyclization events that occur in type II PKS pathways. These transformations have long been unclear, as the intractable and spontaneous cyclization of ketide intermediates (Figure 1) have prevented their preparation for detailed studies.[8a,15] In particular, we were interested in mimetics that would allow us to probe ACP sequestration as a potential regulating force of substrate transport between elongation and initial cyclization, as illustrated by the conversion of **7** to **8** (Figure 1) by the actinorhodin ketoreductase (KR) as well as the processivity between KR and the aromatase/cyclase (ARO/CYC).[15b]

A central mystery in type II PKS ACP arises during the processing of highly reactive polyketone intermediates to cyclized products, as exemplified by the conversion of **6** to **10** (Figure 1). This process includes steps of cyclization, reduction, and aromatization. We have hypothesized that intermediate stabilization through sequestration of elongated intermediates within the ACP may play a role during this transformation. To test this hypothesis, we recently demonstrated that actACP binds mature tricyclic product analogs between helices II and IV.[12] Crump and co-workers decisively showed that simple di- and triketide analogs are not sequestered by actACP,[7a,16] but linear hydrocarbons do bind within the protein. Taken together, these findings indicate that identity of the intermediates likely plays a major role in substrate translocation between enzymes. As demonstrated above, the presence of polar residues such as D62 and D63 on helix III may stabilize the polar nature of polyketone intermediates and may be better suited to the environment of the actACP interior cavity. But what about the monocyclic product of the KR? Is this species directly routed to the ARO/CYC domain or does it return to the actACP pocket between enzymatic transformations? To address these questions, the preparation of elongated monocyclic probes is critical for further insight into the role of sequestration in type II PKS biosynthesis.

To this end, analogs **8a**−**8c** (Figure 5) were proposed as probes that mimic the structural identity of putative intermediates as a means of evaluating actACP sequestration.

dx.doi.org/10.1021/ja5064857 | J. Am. Chem. Soc. 2014, 136, 16792−16799

Analog **8a** offered the most simplified mimetic by providing a single aromatic ring with six ketide units. Analog **8b** and **8c** more closely resembled the putative intermediate **8** (Figure 1) with the addition of an upstream diketide, where the ketide units extended from six in **8a** and **8b** to eight in **8c**, respectively. Our first goal in this effort was the preparation of **8a**–**8c** for phosphopantetheine attachment to ^{15}N-enriched actACP for solution-phase protein NMR studies of substrate sequestration.

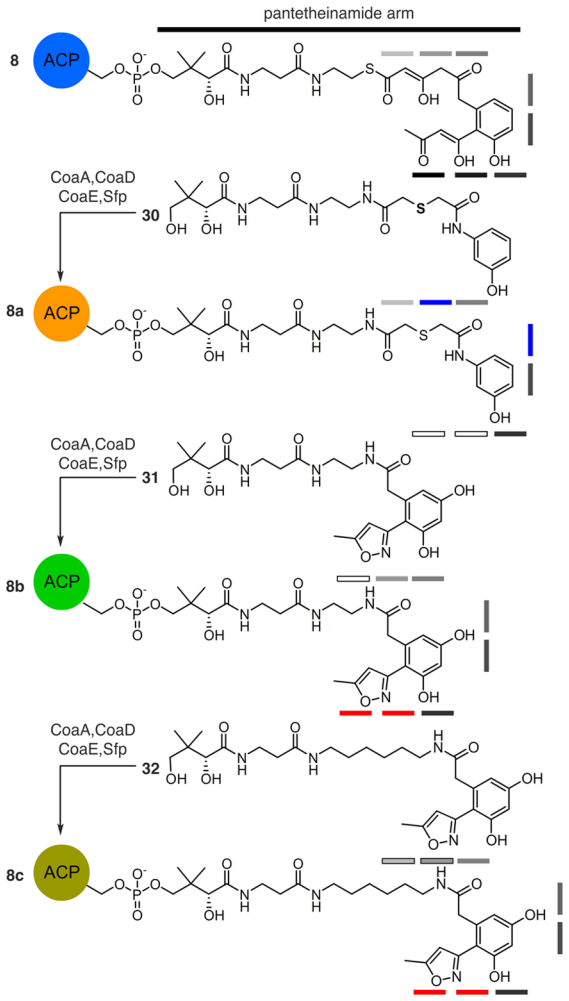

Figure 5. Structures of atom replaced *crypto*-actACP **8a**, **8b**, and **8c**. Access to **8a**, **8b**, and **8c** was achieved by chemoenzymatic conversion of mimetics **30**, **31**, and **32**, respectively, to their corresponding CoA analogs by the action three *E. coli* enzymes CoaA, CoaD, CoaE,[10] followed by loading on the actACP by Sfp (see Supporting Information).[11] Mimetic **30** contains N and S atom replacement (blue bars) and bears structural truncation (black-outlined bars). In mimetics **31** and **32**, 1,3-dicarbonyl units are replaced by isoxazole (red bars). Two different length substrates were examined. Shaded gray bars denote ketide units.

We began with the preparation of **8a** by application of hexaketide mimic **30**. A general strategy for the synthesis of **30** involves the treatment of *m*-aminophenol (**33**) with thiodiglycolic anhydride (**34**) to provide aromatic acid **35** (Scheme 3). Acid **35** was then coupled to protected pantetheinamine **18** to afford **36**. Amide **36** was then deprotected by using aqueous acetic acid to deliver mimetic **30** in 19% overall yield from **33**. While **30** was readily accessed, it lacks two of the terminal ketides (black-outlined boxes, Figure 5). We next explored

Scheme 3. Synthesis of Mimetic 30[a]

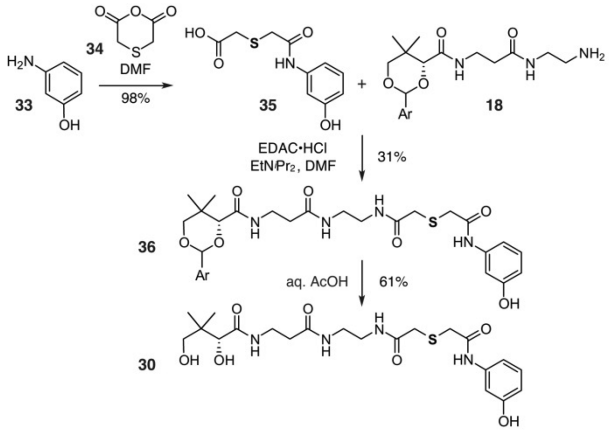

[a]Ar = 4-methoxyphenyl.

mimetics **31** and **32** that provide approximate isosteric placement of this additional diketide moiety. As depicted in Figure 5, these materials expanded on our use of an isoxazole as a diketide mimetic.

We then turned to the preparation of **8b** and **8c** from the respective mimetics **31** and **32** (Figure 5). The synthesis of mimetics **31** (Scheme 4) and **32** (Scheme 5) arose through preparation of acid **41** as a central intermediate. Application of a Vilsmeier–Haak formylation to **37**[17] produced crystalline **38** in excellent yield. Aldehyde **38** was converted to its corresponding oxime **39**, which was then subjected to a 1,3-dipolar cycloaddition with isopropenyl acetate to afford isoxazole **40**. Preparation of acid **41** was then completed by hydrolysis under basic conditions.

Two additional steps were required to complete the synthesis of mimetic **31** (Scheme 4). Acid **41** was coupled to protected-pantetheinamine **18** to deliver amide **42**. Global deprotection under conventional hydrogenation conditions provided **31** in 15% overall yield from **37**. While mimetic **31** contained the missing diketide unit from **30** (Figure 5), its chain length did not

Scheme 4. Synthesis of Mimetic 31[a]

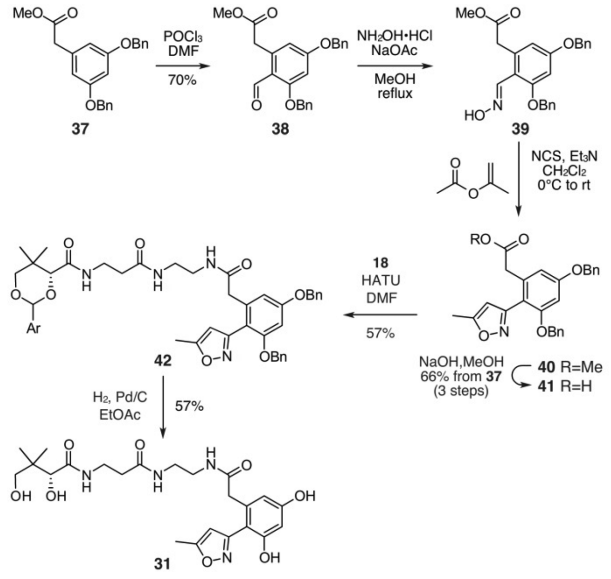

[a]Ar = 4-methoxyphenyl.

dx.doi.org/10.1021/ja5064857 | J. Am. Chem. Soc. 2014, 136, 16792–16799

match that of the putative intermediate **8** (Figure 5). We therefore prepared a third mimetic **32** (Scheme 5) through the addition of a six-carbon spacer.

Scheme 5. Synthesis of Mimetic 32[a]

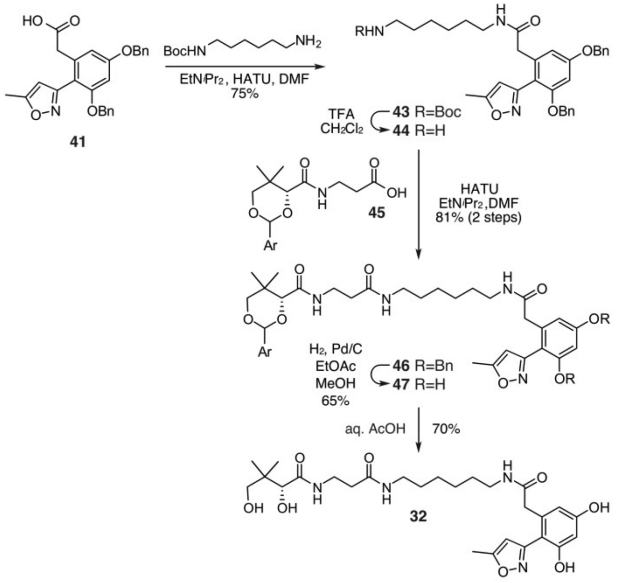

[a]Ar = 4-methoxyphenyl.

Advantageously, acid **41** could be used to prepare a chain-elongated mimetic **32** (Scheme 5). This began by preparing amide **43** by coupling *N*-Boc-1,6-hexanediamine to **41**. Boc-deprotection followed by coupling of amine **44** to protected pantothenic acid **45** afforded amide **46**. A two-step sequence involving deprotection of the benzyl ethers in **46**, followed by removal of the PMP acetal in **47** under acidic conditions, provided mimetic **32** in 13% overall yield from **41**.

We then loaded mimetics **30**-**32** to ^{15}N-enriched actACP chemoenzymatically as previously reported[10−12] to generate *crypto*-actACP **8a**, **8b**, and **8c**, respectively. Next, we subjected *crypto*-actACP **8a**−**8c** to solution-phase protein NMR studies (Figure 6a). CSPs were observed (Figure 6b), which compare the *crypto*-actACP **8a**−**8c** to *holo*-actACP. We found that the *crypto*-actACP loaded with cyclized hexaketide mimetic **30** showed slight CSPs; the *crypto*-actACP loaded with cyclized mimetic **31** showed moderate CSPs; and the *crypto*-actACP loaded with cyclized mimetic **32** showed large CSPs in residues important to the interior sequestration cavity of actACP (Figure 6).[12]

On the NMR time scale, the fully elongated, cyclized octaketide **32** had much higher residence time in the actACP interior cavity than **30** or **31**. The strongest perturbations were observed in residues located at the end of helix III and the following loop, which corroborate with the sequestration residues that we previously reported in emodin-*crypto*-ACP.[12] Interestingly, only species **8c** showed moderate periodic perturbations throughout residues in helix II and those

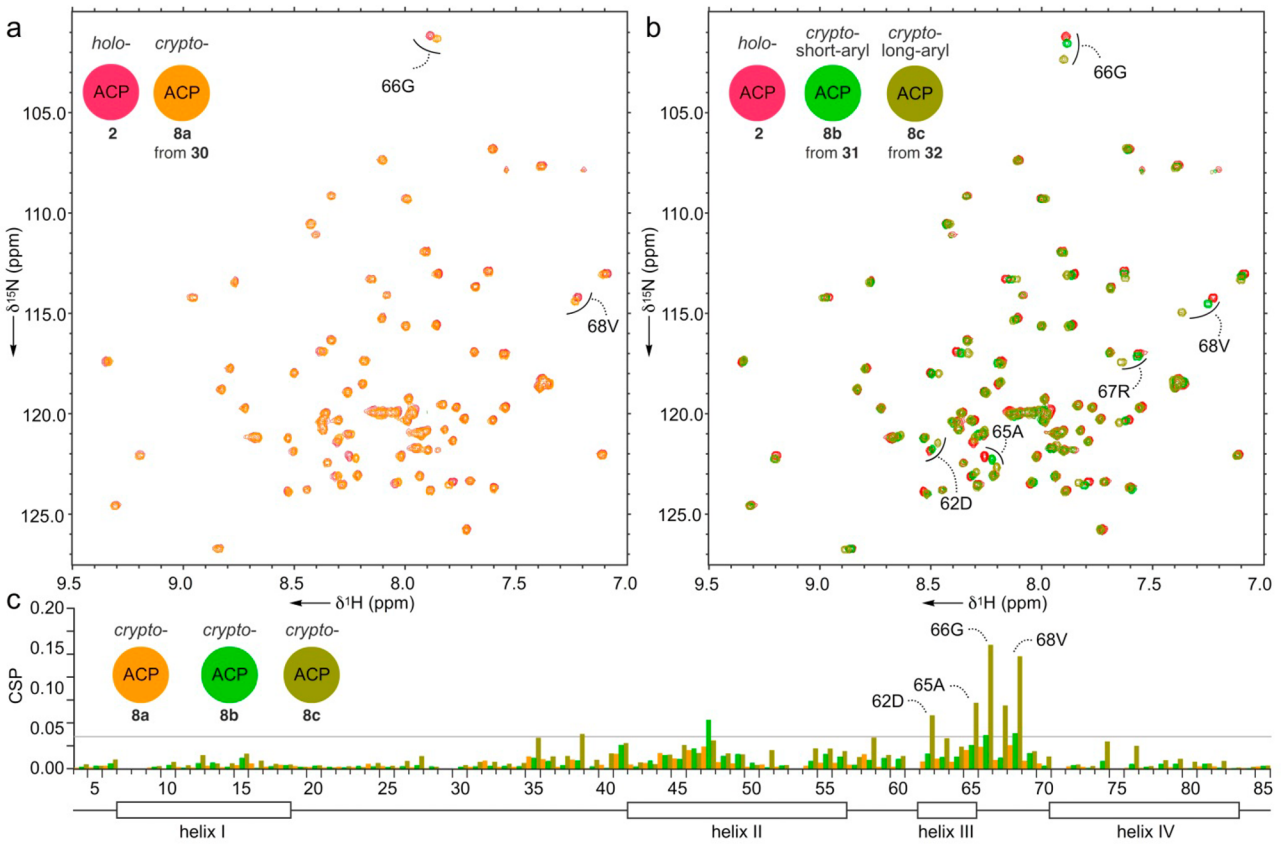

Figure 6. Sequestration analysis of atom replaced cyclic intermediates. (a) ^{1}H,^{15}N-HSQC traces depicting overlays of the *holo*-actACP (**2**, red) and the *crypto*-actACP (**8a**, orange) bearing hexaketide mimetic **30** (Figure 5). (b) ^{1}H,^{15}N-HSQC traces depicting overlays of the *holo*-actACP (**2**, red), *crypto*-actACP (**8b**, green) bearing hexaketide mimetic **31** and *crypto*-actACP (**8c**, brown) bearing octaketide mimetic **32**. (c) CSP plots obtained from the spectra shown in panels (a and b).

dx.doi.org/10.1021/ja5064857 | J. Am. Chem. Soc. 2014, 136, 16792−16799

immediately preceding it. This information mirrored our study on linear polyketide mimetics (Figure 4), which showed the strongest sequestration of the fully elongated mimetic **32**.

In this study, we have shown that selective replacement of carbonyl groups with heteroatoms facilitates access to a diverse class of polyketide mimetics that can be used to interrogate polyketide biosynthetic enzymes. Inherent to this methodology, these atom replacement mimetics can be chemoenzymatically conjugated to ACP through the corresponding CoA analogs, which provide the native scaffold to study these processes. While no probe could ever exactly mimic the properties of natural polyketone intermediates, this work demonstrates that molecules that are much more polar than fatty acids[14c] or tricyclic aromatics[12] do associate with actACP, that longer chains experience more residence time, and that cyclic intermediates demonstrate the longest residence times. Our data, combined with docking simulation of these probes (Figure S34), strongly support that binding of both linear and cyclized polyketide mimetics is not observed unless the mimetics are of sufficient length. Taken together, these observations suggest that until the polyketide has reached its terminal length, no preferential sequestration by the actACP stabilizes the intermediate. However, at full elongation, polyketide binding with the actACP could facilitate release from the ketosynthase and assist transfer to the KR for the first cyclization and reduction steps.[15b] Binding of the first cyclized, reduced intermediate by the actACP would then occur to facilitate release from the KR, followed by delivery to the ARO/CYC.

In this study, the goal of these atom replacement mimetics was to help understand the comparative binding and stabilization of polyketone intermediates by ACPs. These mimetics were not designed to serve as functional substrates of PKS enzymes but instead to mimic the length, polarity, and hydrophobicity found in natural intermediates. As with all mimetics, the match was not perfect. In these examples, the C–S bonds are considerably longer than those of their anticipated ketides. The actual enol-keto states of natural polyketones remain unknown, and the isoxazole moiety in part restricts conformational freedom. These caveats aside, the establishment of polyketide mimietics provides an excellent tool for interrogating the iterative processes polyketide biosynthesis.

Finally, the involvement of the ACP in these pathways adds significant complexity when compared to non-templated biosynthetic pathways, and the creation of new tools to understand this role merits special attention. Most critically, this study defines new methods of atom replacement that can be used to rapidly assemble both linear and cyclic polyketide mimetics for structural and functional applications. Studies on the protein–protein interactions of these species are ongoing.

■ ASSOCIATED CONTENT

Supporting Information

Copies of spectral data, synthetic methods, and experimental procedures. This material is available free of charge via the Internet at http://pubs.acs.org.

■ AUTHOR INFORMATION

Corresponding Authors

sctsai@uci.edu
mburkart@ucsd.edu

Author Contributions

[§]G.S. and H.R. contributed equally.

Notes

The authors declare no competing financial interest.

■ ACKNOWLEDGMENTS

We thank Dr. X. Huang (UCSD), Dr. A. Mrse (UCSD), Dr. Y. Su (UCSD), and Dr. P. Dennison (ICI) for assistance with collection of NMR and MS data. We also thank Prof. C. A. Townsend (Johns Hopkins), Prof. F. Ishikawa (UCSD), Prof. C. D. Vanderwal (UCI), and Prof. A. R. Chamberlin (UCI) for helpful advice. We also thank Prof. M. P. Crump for your advices from full structural determinations as well as helpful discussions. Funding was provided by National Institutes of Health GM100305 and GM095970.

■ REFERENCES

(1) (a) Sadler, P. A.; Eschenmoser, A.; Scheinz, H.; Stork, G. *Helv. Chem. Acta* **1957**, *40*, 2191. (b) Stork, G.; Burgstahler, A. W. *J. Am. Chem. Soc.* **1955**, *77*, 5068. (c) Ruzicka, L.; Eschenmoser, A.; Heusser, H. *Experientia* **1953**, *9*, 357. (d) Ruzicka, L. *Experientia* **1954**, *50*, 1.

(2) Abe, I.; Rohmer, M.; Prestwich, G. D. *Chem. Rev.* **1993**, *93*, 2189.

(3) (a) Johnson, W. S.; Semmelhack, M. F.; Sultanbawa, M. U.; Dolak, L. A. *J. Am. Chem. Soc.* **1968**, *90*, 2994. (b) Schmidt, R.; Huesmann, P. L.; Johnson, W. S. *J. Am. Chem. Soc.* **1980**, *102*, 5122.

(4) (a) Pichersky, E.; Noel, J. P.; Dudareva, N. *Science* **2006**, *311*, 808. (b) Yoder, R. A.; Johnston, J. N. *Chem. Rev.* **2005**, *105*, 4730. (c) Poralla, K. *Chem. Biol.* **2004**, *11*, 12. (d) Xu, R.; Fazio, G. C.; Matsuda, S. P. *Phytochemistry* **2004**, *65*, 261.

(5) (a) Akey, D. L.; Gehret, J. J.; Khare, D.; Smith, J. L. *Nat. Prod. Rep.* **2012**, *29*, 1038. (b) Crawford, J. M.; Townsend, C. A. *Nat. Rev. Microbiol.* **2010**, *8*, 870. (c) Khosla, C. *J. Org. Chem.* **2009**, *74*, 6416. (d) Das, A.; Khosla, C. *Acc. Chem. Res.* **2009**, *42*, 631. (e) Bumpus, S. B.; Kelleher, N. L. *Curr. Opin. Chem. Biol.* **2008**, *12*, 475.

(6) (a) Korman, T. P.; Hill, J. A.; Vu, T. N.; Tsai, S. C. *Biochemistry* **2004**, *43*, 14529. (b) Rudd, B. A.; Hopwood, D. A. *J. Gen. Microbiol.* **1979**, *114*, 35. (c) Fernández-Moreno, M. A.; Martínez, E.; Caballero, J. L.; Ichinose, K.; Hopwood, D. A.; Malpartida, F. *J. Biol. Chem.* **1994**, *269*, 24854.

(7) (a) Crump, M. P.; Crosby, J.; Dempsey, C. E.; Parkinson, J. A.; Murray, M.; Hopwood, D. A.; Simpson, T. J. *Biochemistry* **1997**, *36*, 6000. (b) Revill, W. P.; Bibb, M. J.; Hopwood, D. A. *J. Bacteriol.* **1996**, *178*, 5660.

(8) (a) Teufel, R.; Miyanaga, A.; Michaudel, Q.; Stull, F.; Louie, G.; Noel, J. P.; Baran, P. S.; Palfey, B.; Moore, B. S. *Nature* **2013**, *503*, 552. (b) Ames, B. D.; Lee, M. Y.; Moody, C.; Zhang, W.; Tang, Y.; Tsai, S. C. *Biochemistry* **2011**, *50*, 8392. (b1) Tsai, S. C.; Lu, H.; Cane, D. E.; Khosla, C.; Stroud, R. M. *Biochemistry* **2002**, *41*, 12598. (c) Pan, H.; Tsai, S. C.; Meadows, E. S.; Miercke, L. J.; Keatinge-Clay, A. T.; O'Connell, J.; Khosla, C.; Stroud, R. M. *Structure* **2002**, *10*, 1559.

(9) (a) Fouché, M.; Rooney, L.; Barrett, A. G. M. *J. Org. Chem.* **2012**, *77*, 3060. (b) Calo, F.; Richardson, J.; Barrett, A. G. M. *Org. Lett.* **2009**, *11*, 4910. (c) Navarro, I.; Basset, J. F.; Hebbe, S.; Major, S. M.; Werner, T.; Howsham, C.; Bräckow, J.; Barrett, A. G. M. *J. Am. Chem. Soc.* **2008**, *130*, 10293. (d) Harris, T. M.; Murray, T. P.; Harris, C. M.; Gumulka, M. *J. Chem. Soc. Chem. Comm.* **1974**, *10*, 362. (e) Harris, T. M.; Harris, C. M. *Tetrahedron* **1977**, *33*, 2159.

(10) (a) Worthington, A. S.; Burkart, M. D. *Org. Biomol. Chem.* **2006**, *4*, 44. (b) Kosa, N. M.; Haushalter, R. W.; Smith, A. R.; Burkart, M. D. *Nat. Methods* **2012**, *9*, 981.

(11) (a) La Clair, J. J.; Foley, T. L.; Schegg, T. R.; Regan, C. M.; Burkart, M. D. *Chem. Biol.* **2004**, *11*, 195. (b) Meier, J. L.; Burkart, M. D. *Methods Enzymol.* **2009**, *458*, 219. (c) Foley, T. L.; Burkart, M. D. *Curr. Opin. Chem. Biol.* **2007**, *11*, 12.

(12) Haushalter, R. W.; Filipp, F. V.; Ko, K. S.; Yu, R.; Opella, S. J.; Burkart, M. D. *ACS Chem. Biol.* **2011**, *6*, 413.

(13) (a) Stork, G.; Hagedorn, A. A., III *J. Am. Chem. Soc.* **1978**, *100*, 3609. (b) Stork, G.; La Clair, J. J.; Spargo, P.; Nargund, R. P.; Totah, N. *J. Am. Chem. Soc.* **1996**, *118*, 5304. (c) Wright, P. M.; Myers, A. G.

Tetrahedron **2011**, *67*, 9853. (d) Sun, C.; Wang, Q.; Brubaker, J. D.; Wright, P. M.; Lerner, C. D.; Noson, K.; Charest, M.; Siegel, D. R.; Wang, Y. M.; Myers, A. G. *J. Am. Chem. Soc.* **2008**, *130*, 17913. (e) Charest, M. G.; Siegel, D. R.; Myers, A. G. *J. Am. Chem. Soc.* **2005**, *127*, 8292.

(14) (a) Roujeinikova, A.; Simon, W. J.; Gilroy, J.; Rice, D. W.; Rafferty, J. B.; Slabas, A. R. *J. Mol. Biol.* **2007**, *365*, 135. (b) Płoskoń, E.; Arthur, C. J.; Kanari, A. L.; Wattana-amorn, P.; Williams, C.; Crosby, J.; Simpson, T. J.; Willis, C. L.; Crump, M. P. *Chem. Biol.* **2010**, *17*, 776. (c) Evans, S. E.; Williams, C.; Arthur, C. J.; Płoskoń, E.; Wattana-amorn, P.; Cox, R. J.; Crosby, J.; Willis, C. L.; Simpson, T. J.; Crump, M. P. *J. Mol. Biol.* **2009**, *389*, 511.

(15) (a) Nguyen, C.; Haushalter, R. W.; Lee, D. J.; Markwick, P. R.; Bruegger, J.; Caldara-Festin, G.; Finzel, K.; Jackson, D. R.; Ishikawa, F.; O'Dowd, B.; McCammon, J. A.; Opella, S. J.; Tsai, S. C.; Burkart, M. D. *Nature* **2014**, *505*, 427. (b) Javidpour, P.; Bruegger, J.; Srithahan, S.; Korman, T. P.; Crump, M. P.; Crosby, J.; Burkart, M. D.; Tsai, S. C. *Chem. Biol.* **2013**, *20*, 1225.

(16) Revill, W. P.; Bibb, M. J.; Hopwood, D. A. *J. Bacteriol.* **1996**, *178*, 5660.

(17) Marsini, M. A.; Pettus, T. R. R.; Wenderski, T. A. *Org. Lett.* **2011**, *13*, 118.